Journal of Energy Storage 129 (2025) 117274

Contents lists available at ScienceDirect

Journal of Energy Storage

journal homepage: www.elsevier.com/locate/est

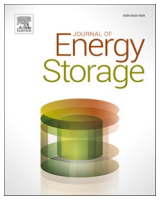

Research papers

Impact of CO_2 impurity in hydrogen gas on wetting characteristics of carbonate minerals; new insights and implications for hydrogen geo-storage in saline aquifers

Amirmansour Jafari [a], Zoha Dalal Isfehani [b], Jalal Fahimpour [c,*], Nima Shokri [d], Mirhasan Hosseini [e], Mohammad Sharifi [a]

[a] Department of Petroleum and GeoEnergy Engineering, Amirkabir University of Technology, Tehran, Iran
[b] Department of Civil and Environmental Engineering, Hamburg University of Technology, Hamburg, Germany
[c] Institute of GeoEnergy Engineering, Heriot-Watt University, Edinburgh, UK
[d] Institute of Geo-Hydroinformatics, Hamburg University of Technology, Hamburg, Germany
[e] Petroleum Engineering Discipline, School of Engineering, Edith Cowan University, Australia

ARTICLE INFO

Keywords:
Hydrogen geo-storage
Carbonate mineral
Wettability
Cushion gas
Contact angle
Carbon dioxide

ABSTRACT

The effectiveness of Underground Hydrogen Storage (UHS) as a long-term solution for sustainable green energy relies on secure containment in geological formations and optimized storage and retrieval processes, where fluid-rock interactions, particularly the wettability of the rock, play a crucial role. Additionally, the pre-injection of a cushion gas, such as CO_2, to maintain sufficient pressure for hydrogen (H_2) withdrawal can influence wettability. This study employed the tilted plate method to examine contact angle hysteresis of the wetting phase (water) on a carbonate rock substrate, measuring advancing and receding contact angles in the presence of various H_2-CO_2 mixtures ([0.30 CO_2 + 0.70 H_2], [0.50 CO_2 + 0.50 H_2, 0.70 CO_2 + 0.30 H_2]) at pressures (500, 1200, 2000, and 3000 psi) and temperatures (50 °C and 80 °C). Further analyses using AFM (Atomic Force Microscopy) and EDS (Energy Dispersive X-ray Spectroscopy) were conducted to assess the effects of CO_2 impurity on the carbonate rock surface. Our findings indicate that while pressure has minimal effect on the wetting properties of the carbonate substrate, higher temperatures make the surface more water-wet. More importantly, CO_2 concentration plays a critical role in system wettability, as increasing the CO_2 mole fraction from 30 % to 70 % significantly reduces the water-wetness of the carbonate surface. Specifically, the rock remains water-wet under reservoir conditions when CO_2 is 50 % or less, with contact angles between 42° and 65°, whereas at higher CO_2 levels, it shifts toward neutral wettability, with contact angles ranging from 80° to 100°. AFM and EDS analyses indicate that changes in surface roughness and elemental concentration due to CO_2 exposure contribute to these wettability variations. As a result, at lower CO_2 concentrations because of more water-wet state of the surface and higher IFT, a higher gas column height and storage capacity is acheivable, whilst stronger snap-off effect and hence more trapped gas during water imbibition process, impairs the hydrogen recovery efficiency. The opposite applies at higher CO_2 levels. Thus, optimizing CO_2 concentration is a key factor in balancing the storage capacity and the recovery efficiency. The findings of this work enhance our understanding of hydrogen geo-storage mechanisms in carbonate reservoirs with CO_2 as a cushion gas, supporting more reliable predictions for underground hydrogen storage projects.

1. Introduction

In recent decades, renewable energy has gained significant attention for its contribution to adaptation and mitigation efforts aimed at combating global warming and climate challenges [1,2]. However, to meet energy security and sustainability requirements, any renewable energy source must support long-term storage to balance supply and demand [2–4]. In this regard, there has been a growing effort to develop hydrogen storage as a renewable energy solution due to its potential for decarbonization [3,5]. However, storing hydrogen is a significant

* Corresponding author.
E-mail address: j.fahimpour_1@hw.ac.uk (J. Fahimpour).

https://doi.org/10.1016/j.est.2025.117274
Received 30 September 2024; Received in revised form 18 May 2025; Accepted 30 May 2025
Available online 10 June 2025

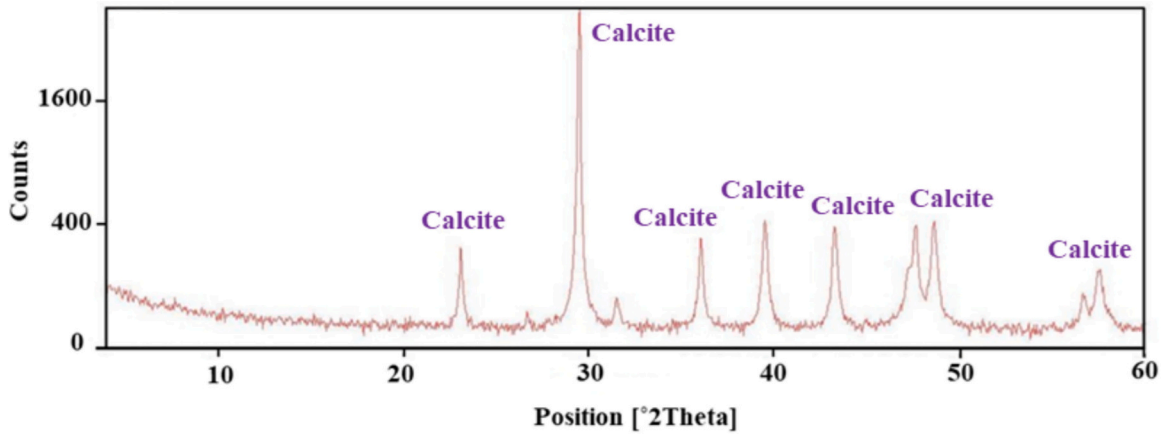

Fig. 1. XRD pattern of the used carbonate rock.

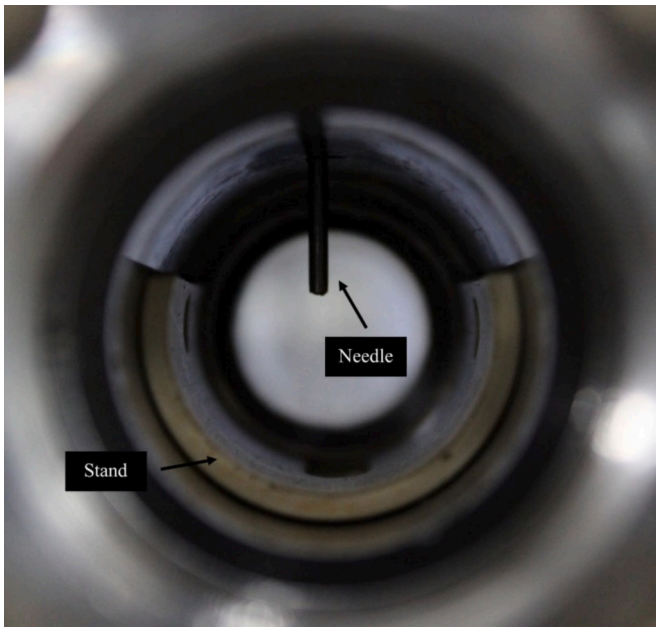

Fig. 2. Internal view of the HPHT Optical view chamber.

challenge due to its highly compressible and volatile nature [6,7]. Surface-based storage facilities, such as pipelines and tanks, have limited storage and discharge capacity. By contrast, employment of subsurface geosystems would provide a practical and safe solution for large-scale hydrogen storage. As a result, underground hydrogen storage in the salt caverns and geological formations, e.g. depleted hydrocarbon reservoirs, and saline aquifers, can provide a long-term storage system [5,6,8,9]. In addition, the utilization of UHS enhances safety by eliminating atmospheric oxygen contact, a crucial factor given the potential explosiveness of hydrogen-oxygen mixture [10]. Hydrogen can be stored in various forms, for example, pure hydrogen, a mixture with natural gas, and a rich hydrogen mixture with CO, CH_4, and CO_2 [10] or in an aquifer with cushion gas support. The aquifer needs to have adequate porosity and permeability to contain a significant amount of hydrogen with a trapping mechanism, like a sealing cap rock [11]. The hydrogen purity levels vary depending on the storage location. For instance, salt caverns, aquifers, and depleted gas reservoirs could contain pure, less pure, and the least pure hydrogen, respectively [10,12].

In UHS, hydrogen is injected via a wellbore into the geological structure, where it can be withdrawn or refilled many times [6,13]. One of the vital parameters in gas storage is rock wettability, which is crucial for determining fluid flow and distribution within the porous rock that can be described by parameters such as residual saturation, capillary pressure, and relative permeability [6,14]. The wettability is controlled by various geological and thermodynamic factors such as surface chemistry, reservoir pressure, temperature, water salinity, and ion type [15].

Cushion gas is initially injected into the aquifer and cavern storage systems to provide the necessary pressure for gas injection and retrieval. Its presence is essential in all underground gas storage operations, ensuring the proper functioning of the storage process. The required amount of cushion gas varies depending on the storage method. For example, cushion gas typically accounts for about 50 % of the total volume in depleted gas reserves, whereas salt caverns generally require around 25 %. Aquifer reservoirs, on the other hand, may need up to 80 % of their total capacity. In short, the exact amount of cushion gas required depends on the specific storage conditions and withdrawal rates [16]. In hydrocarbon gas storage operations, typically both the working gas and cushion gas have similar compositions [17]. For UHS applications, however, using non-hydrogen gas like CH_4, N_2, or CO_2, instead of hydrogen, as cushion gas can potentially reduce storage costs and greenhouse gas emissions. Using such alternatives for natural gas storage has already shown promising results [18–21]. Choosing a proper cushion gas for UHS is influenced by several factors such as gas cost and physical properties [22]. In this regard, CO_2 has been utilized in various applications, including Enhanced Oil Recovery (EOR), where CO_2 is injected into oil reservoirs to increase production. It is also used in the extraction of natural gas from methane hydrates through a process that replaces methane with CO_2, enabling the extraction of natural gas from these abundant resources. Additionally, CO_2 plays a key role in long-term storage and sequestration projects to mitigate its environmental impact [23].

Some studies have indicated that carbon dioxide has a significant impact on surface properties and wettability of rock surfaces. Contact angle experiments have shown wettability alternation of hydrophilic surfaces to almost neutral-wet conditions, after being in contact with CO_2 either in its pure form [24–27] or in combination with other gases such as hydrogen, methane, or nitrogen. The results from core flooding experiments [28] on water-wet sandstone before and after supercritical CO_2 injection revealed that carbon dioxide had no impact on the system's wettability. On the other hand, the data from another study [29] indicated that the transition of wettability from a strongly water-wet to a neutral water-wet state occurred exclusively in muscovite mica samples, whereas the calcite samples exhibited negligible alteration in wettability.

CO_2 can also be used as a promising cushion gas, providing the added benefit of storing CO_2 emissions in subsurface geological formations.

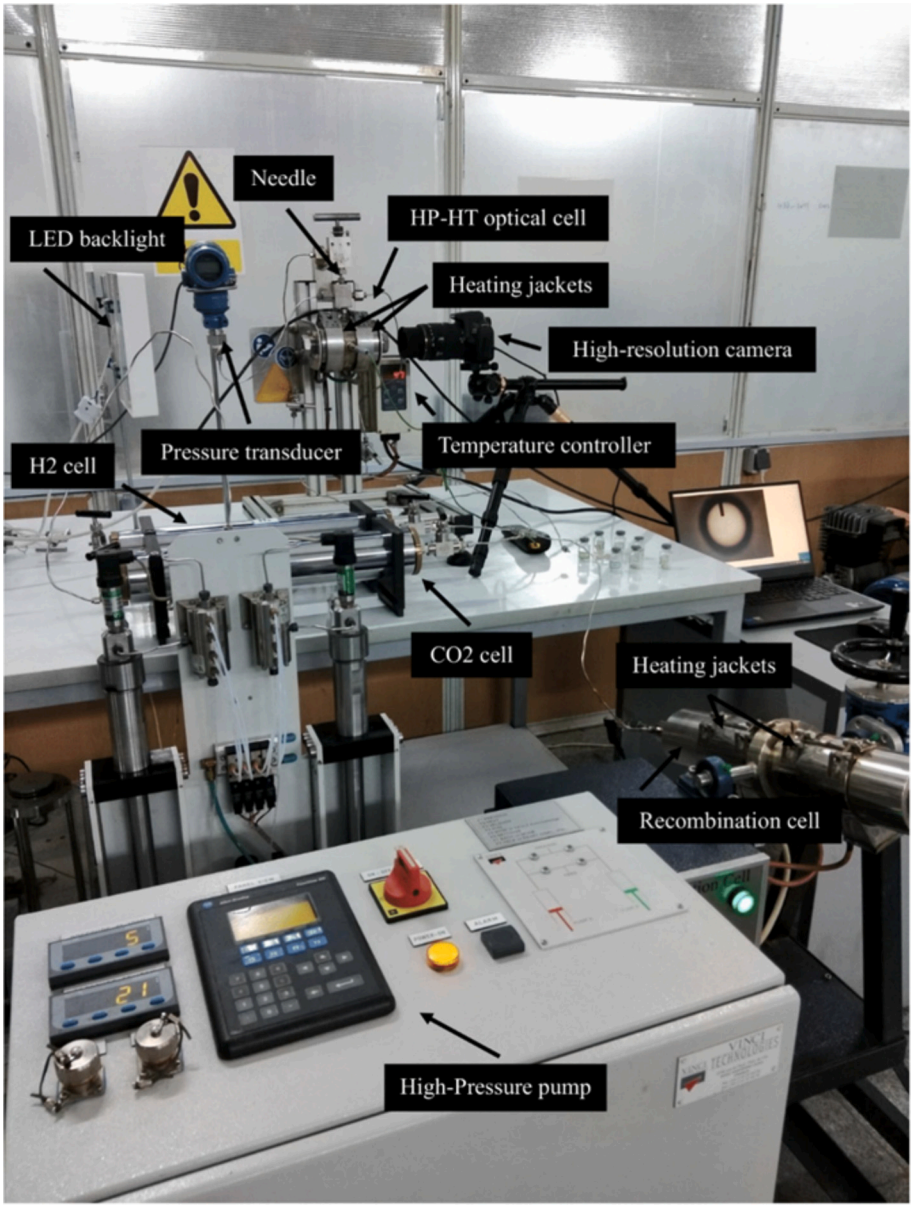

Fig. 3. The experimental setup used for contact angle measurements.

The wettability of the H_2/brine/rock system in the presence of CO_2 as a cushion gas has been studied in the past, but the research remains insufficient and leaves critical uncertainties. It has not covered every type of rock and, importantly, has never been conducted for carbonate rocks. For instance, Ali et al. [30] investigated the impact of CO_2 and CH_4 concentration on the wettability of kaolinite surface in H_2/brine system. Their results showed that cushion gases, specifically CO_2, make the surface less water-wet. Another research by Ali et al. (2021) studied the wettability of mica and quartz surfaces in H_2/brine and CO_2/brine systems at 323 K and 20 MPa [31]. While mica showed to be weakly water-wet in presence of H_2, it became intermediate-wet when exposed to CO_2. To assess the impact of hydrogen gas on wettability changes, Hashemi et al. (2021) investigated the contact angle measurements using the captive bubble method under varying pressures, temperatures, and salinity levels. They found that in sandstone samples, no clear trend was observed in the contact angle values of the hydrogen/liquid/sandstone system as a function of pressure, temperature, and salinity variations [32]. Also, our previous work [33] was conducted to investigate the effect of carbon dioxide gas in combination with hydrogen gas on wettability changes of sandstone. By examining various percentages of carbon dioxide in the $CO_2 + H_2$/brine/sandstone system at the different pressures and temperatures, it was observed that the wettability of the system did not undergo significant changes.

In a study by [34], various gas mixtures, including 20–80 % and 80–20 % ratios of hydrogen and nitrogen with fixed 5 % carbon dioxide and methane, were tested to assess wettability using the sessile drop method on sandstone samples. The experiments, conducted under high temperature, high pressure, and varying salinity, revealed that all gas mixtures demonstrated strong water-wet conditions. Contact angles were observed to increase with reservoir pressure and salinity but decrease with rising temperature. Notably, higher contact angle values were associated with a greater nitrogen fraction in the gas mixtures, suggesting that a higher hydrogen fraction could improve structural trapping and enhance containment effectiveness [35]. Another study by [36] investigated the wettability of sandstone rock in the presence of a gas mixture of H_2 and CO_2, under the same conditions as their previous study. Their findings revealed that higher hydrogen fractions resulted in lower contact angles, indicating enhanced residual trapping within the

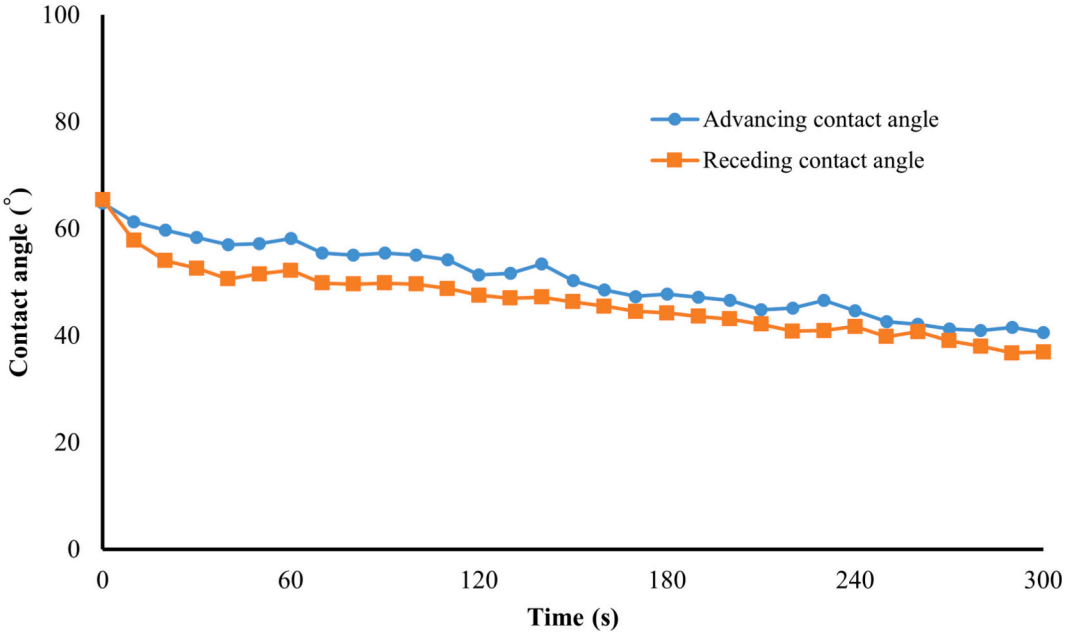

Fig. 4. Dynamic contact angle of pure hydrogen/pure water/calcite system at 323 K and 3.5 MPa.

Table 1
The results of contact angle measurements on the carbonate substrate using the $CO_2 + H_2$/brine system under various thermodynamic conditions.

Gas mixture (mole%)	Pressure (psi)	Temperature (°C)	Advancing θ (°)	Receding θ (°)	Drop volume (μL)
70 % CO_2 + 30 % H_2	500	50	97.7	89.4	5.15
	500	80	80.1	74.8	5.04
	1200	50	96.7	93.8	5.12
	1200	80	78.3	73.3	5.58
	2000	50	99.6	94.5	4.66
	2000	80	80.5	75.7	5.17
	3000	50	98.2	91.1	4.45
	3000	80	84.2	77.0	4.69
50 % CO_2 + 50 % H_2	500	50	76.5	72.4	5.29
	500	80	69.4	64.5	4.71
	1200	50	77.8	71.9	4.86
	1200	80	65.4	57.6	4.75
	2000	50	76.4	70.6	4.80
	2000	80	62.3	57.1	5.60
	3000	50	74.2	69.0	5.26
	3000	80	67.7	61.9	4.54
30 % CO_2 + 70 % H_2	500	50	54.6	49.5	4.62
	500	80	41.7	36.1	5.09
	1200	50	52.2	47.5	4.93
	1200	80	37.7	32.4	4.56
	2000	50	53.1	47.9	4.85
	2000	80	38.8	33.5	4.47
	3000	50	56.7	52.3	5.00
	3000	80	44.7	39.5	4.81

reservoir rocks. Consequently, gas recovery is expected to be most effective at the lowest hydrogen fraction [36]. Moreover, [35] assessed the effect of CH_4 as a cushion gas on the wettability of sandstone under high pressure and temperature conditions. They observed that the contact angle remained consistent despite variations in temperature, pressure, and brine salinity across the examined gas compositions. The contact angle consistently indicated a strong water-wet condition [34]. Several studies have also investigated wettability alterations due to cushion gas in UHS using Molecular Dynamics (MD) simulations. [37] investigated the effect of cushion gas on the H_2/brine/clay system under reservoir conditions. Using molecular dynamics simulations, they found that the impact of cushion gas on clay is highly dependent on clay/brine interactions. Moreover, their results indicate that CO_2 and CH_4 generally shift surface wettability away from the initial water-wet state. The study by [38] also demonstrates, using the molecular dynamics method and the LAMMPS software, that in the H_2/brine/shale system under reservoir conditions, an increase in CO_2 and CH_4 concentrations leads to a wettability alteration from a strongly water-wet state to a gas-wet state.

Several studies have also been published, investigating the effect of wettability on hydrogen flow behavior at the pore-scale level through modeling and simulation exercises. Researchers [39] conducted laboratory experiments by applying a drainage process (hydrogen injection) in a micromodel setup under controlled conditions of 35 bar and 37 °C. It was found that, over time, in addition to the reduction in hydrogen saturation due to microbial consumption, wettability alterations, likely caused by bioproducts and bacterial adhesion to solid surfaces, resulted in a shift in the system's wettability from water-wet to neutral water-wet. In another work [40] employing the pore-scale simulations, using the Volume of Fluid (VOF) method, the drainage process was studied in a micromodel framework with varying degrees of heterogeneity under thermodynamic conditions of 10 MPa and 35 °C. The findings indicated that as the wetting characteristics shifted from water-wet to neutral water-wet, the amount of hydrogen in the system during primary drainage increased. This enhancement was primarily attributed to a reduction in capillary pressure. Pore-scale simulations with the Lattice Boltzmann method (LB) [41] were also conducted based on laboratory H_2/brine core flooding tests performed using X-ray micro-CT imaging. They found that a reduction in the relative distribution of surface contact angles toward more hydrophilic conditions led to an increase in capillary pressure and a corresponding decrease in residual hydrogen saturation. Through pore-scale studies using the VOF method [42], it was found that, due to the viscosity contrast between hydrogen and water under hydrophilic wettability conditions, there is an increased likelihood of snap-off events and consequently, greater trapping of hydrogen within the pore spaces. In another pore-scale study [43],flow behavior of the H_2/brine/rock system was simulated using the Lattice Boltzmann method. The results demonstrated that the increased gas trapping and reduced gas phase connectivity occur under conditions of high capillary number and very low contact angles, characteristic of a strongly water-wet system.

Due to the limited research on the effect of cushion gas as fraction on wettability alternation especially CO_2 in carbonate-rich formations and

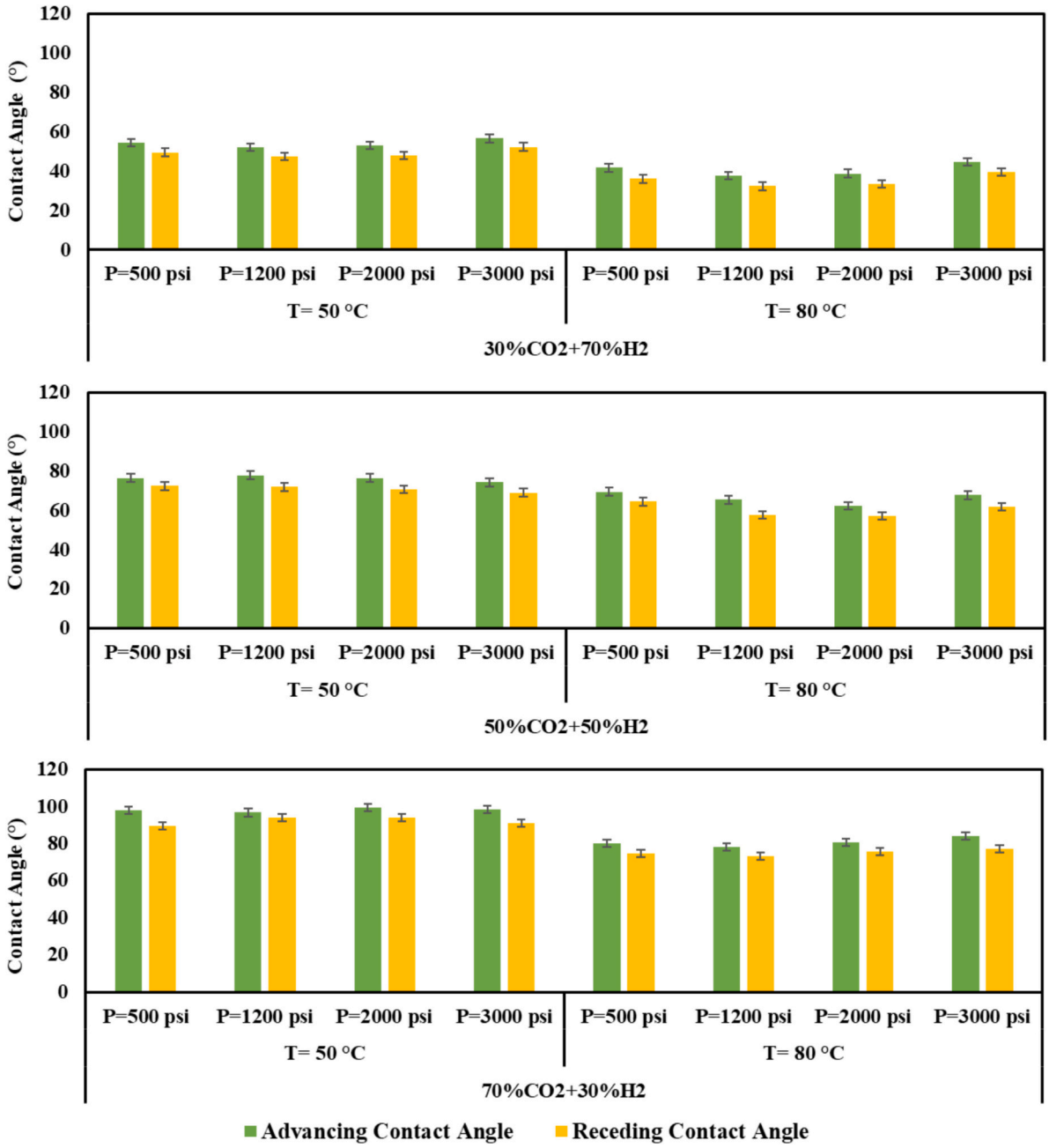

Fig. 5. Experimental data on $CO_2 + H_2$/brine/carbonate rock advancing and receding contact angles as a function of pressure at two temperatures of 50 °C and 80 °C for three gas mixtures of 70 % CO_2 + 30 % H_2, 50 % CO_2 + 50 % H_2, and 30 % CO_2 + 70 % H_2 with error bars indicating the uncertainty in measuring the contact angle using image processing.

the importance of using CO_2 in underground gas storage, our objectives were to investigate and extend the understanding of the impact of CO_2 on wettability alternation of carbonate rock under different pressure and temperature (at geo-storage conditions) in UHS concept using dynamic contact angle method. Consequently, we studied the impact of CO_2 fraction as cushion gas on the wettability of a carbonate rock substrate under different pressures and temperatures used. The receding and advancing dynamic contact angles were measured using the tilted plate technique. AFM (Atomic force microscope) and EDS (Energy Dispersive X-ray Spectroscopy) analyses were also conducted to better scrutinize the impact of CO_2 impurity on carbonate rock surface and its roughness.

2. Experimental methodology

2.1. Materials

Three different mixtures of H_2 and CO_2 were used in this study. The corresponding molar fraction of H_2 in these mixtures is 0.3, 0.5 and 0.7. The mixtures were prepared using pure Hydrogen and Carbon Dioxide, with a purity level greater than or equal to 99 mol%. The brine solution used was a mixture of 1.05 M NaCl (86.4 mol%) and KCl (13.6 mol%) in deionized water with a measured electrical conductivity of 0.02 mS cm^{-1}. The rock substrates were also obtained from a carbonate gas reservoir in Iran with an average porosity and permeability of 15 % and 2 mD, respectively. The rock samples were mainly composed of 98 % calcite, 1 % clay minerals, and <1 % quartz according to the XRD

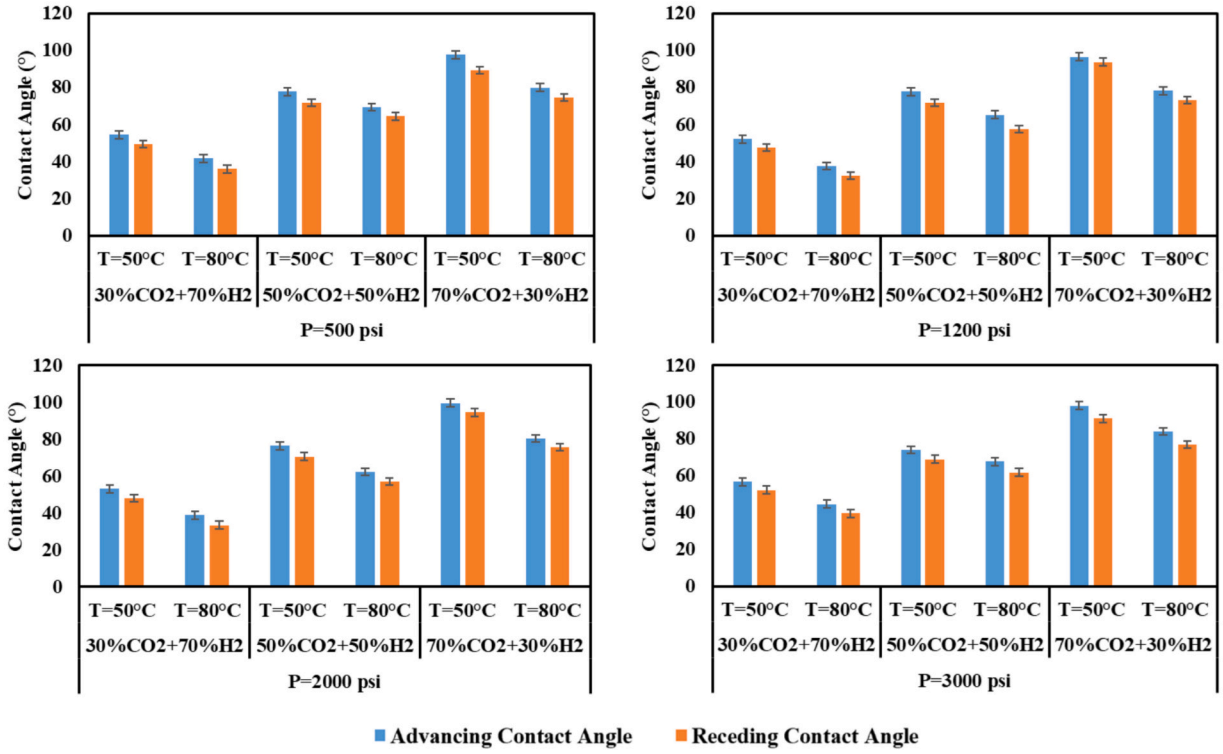

Fig. 6. Experimental data on $CO_2 + H_2$/brine/carbonate rock advancing and receding contact angles as a function of temperature for various H_2 and CO_2 mixtures at pressures of 500, 1200, 2000, and 3000 psi with error bars indicating the uncertainty in measuring the contact angle using image processing.

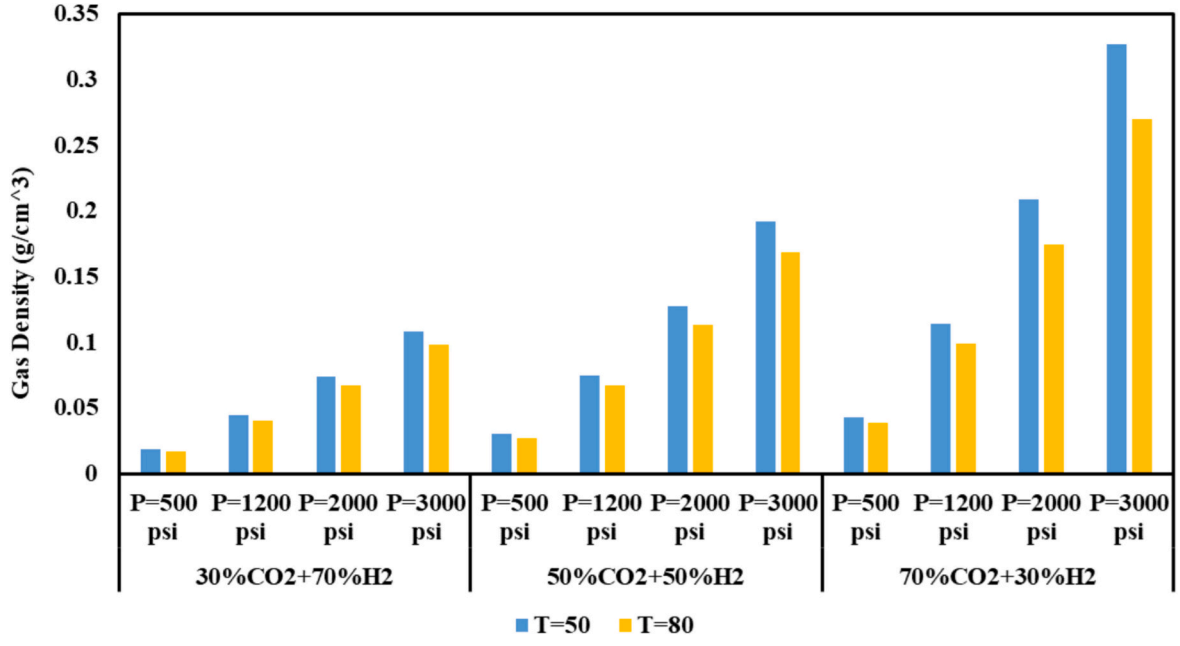

Fig. 7. The density of gas mixture as a function of temperature for various H_2 and CO_2 mixtures at pressures of 500, 1200, 2000, and 3000 psi [64].

analysis (Fig. 1).

2.2. Elemental analysis and surface roughness

Given the impact of surface roughness on wetting characteristics, AFM technique was employed to quantify the roughness of the rock substrates [44]. Geometrical and mathematical parameters are employed to analyse the results of the AFM test. The arithmetic average height parameter (R_a) is characterized as the average absolute deviation of the roughness irregularities from the mean line over one sampling length. The root mean square roughness (R_q), which is also known as RMS, represents the standard deviation of the surface height distribution. This parameter is more sensitive to the deviation from the mean line than R_a. Additionally, the Mean of Maximum Peak to Valley Height (R_{tm}) is characterized by averaging all maximum peak to valley heights measured within the profile's assessment length. R_{tm} exhibits greater

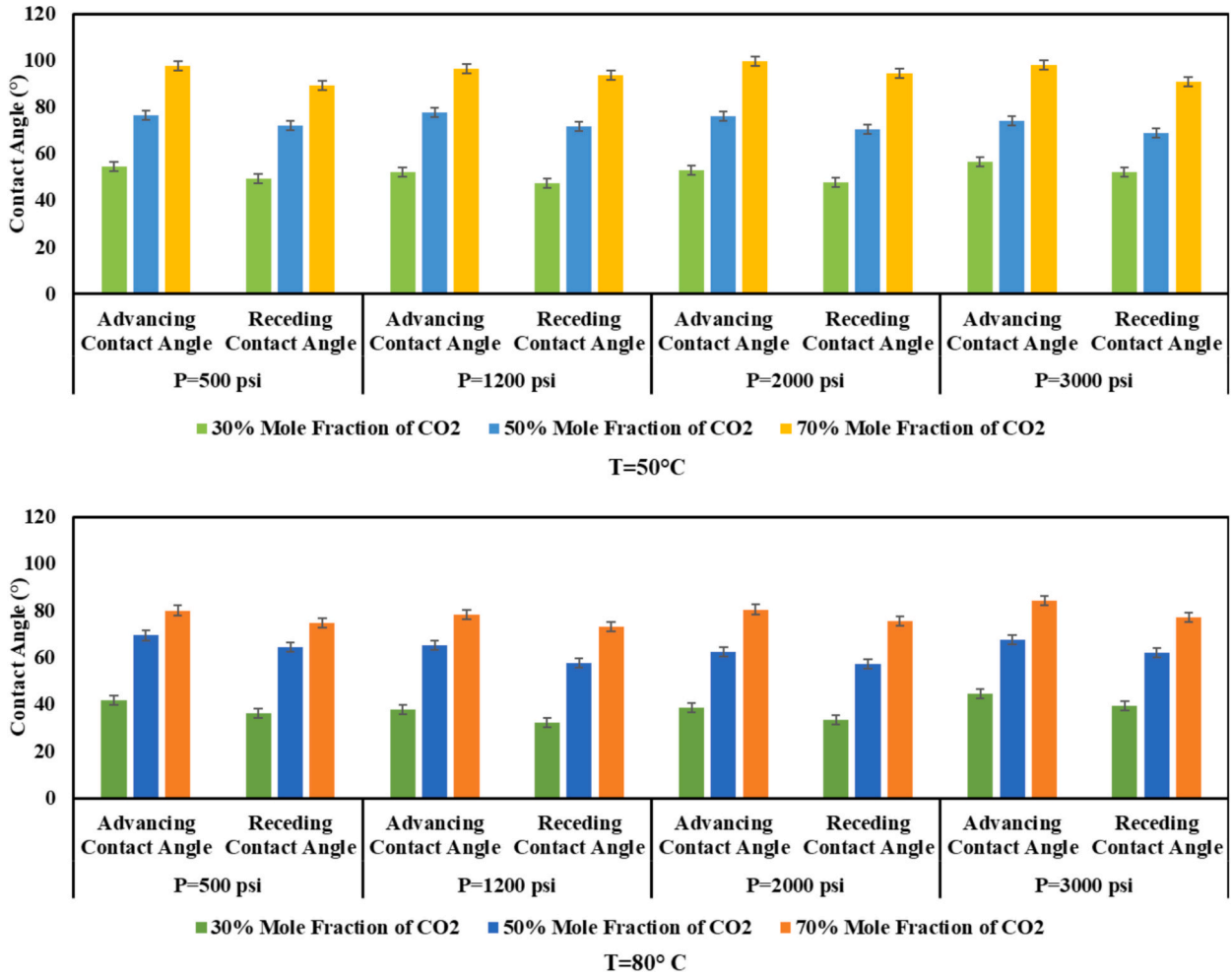

Fig. 8. Experimental data on CO_2+ H_2/brine/carbonate rock advancing and receding contact angles as a function of CO_2 fraction for two temperatures of 50 °C and 80 °C at pressures of 500, 1200, 2000, and 3000 psi.

sensitivity to high peaks or deep valleys in comparison to R_a, similar to the RMS parameter [45].

Moreover, the rock samples went under EDS analyses to detect potential chemical compositional changes caused by exposure to a combination of CO_2 and H_2.

2.3. Experimental procedure

The status of the carbonate rock wettability with respect to different gas mixtures of H_2 and CO_2 was investigated under various pressure and temperature conditions. For this purpose, advancing and receding contact angles were measured using the sessile drop technique for a tilted plate. The tests were performed at four pressures of 500, 1200, 2000, and 3000 psi and two temperatures 50 and 80 °C. First of all, to minimize the risk of contamination affecting the contact angle measurements, the optical cell, its connections, and the needle were thoroughly cleaned with toluene and methanol before each test. They were then completely dried using nitrogen (99.9 mol%), blowing to ensure a clean testing environment.

To perform the tests, rock substrates with a dimension of 1.2 × 1.5 × 0.2 cm were trimmed from the available core plugs. The polished samples were first cleaned by immersing them in methanol solutions and then dried in an oven at 100 °C for 12 h. To remove organic impurities, they underwent 15 min of air plasma treatment, followed by surface smoothing with sandpaper. Finally, before testing, the substrates were soaked in a brine solution for seven days to achieve ionic equilibrium. To maintain equilibrium conditions during testing and eliminate the influence of mass transfer between fluids on the measurements, a small volume of water was injected at the bottom of the cell, beneath the sample plate. Afterward, the rock sample was mounted on a tilted plate inside the high-pressure high-temperature optical cell, shown in Fig. 2. The tilted plate used here forms an angle of 15° relative to the horizontal axis [33,46–49].

The temperature of the drop shape apparatus was finally set at the desired test temperature. Following this, the corresponding gas mixture was transferred to the optical cell and sufficient time was allowed for the system to reach equilibrium. A droplet of the aqueous phase was then injected through the needle tip and placed carefully on the carbonate substrate for corresponding contact angle measurement tests. The real photo of the experimental setup used for these measurements is shown in Fig. 3, and the corresponding schematic diagram is provided in Fig. S1 in the supplementary material for further analysis.

The images of the droplet resting on the substrate were then used to determine the advancing and receding contact angle values. Note that the brine and gas mixtures used for contact angle tests were in direct contact within the recombination transfer vessel at the desired test pressure and temperature for at least 24 h to reach equilibrium. During this process, the vessel was rocked upward and downward occasionally to ensure maximum equilibration was achieved. In addition, it is important to mention that each test was conducted three times to verify the consistency and accuracy of the measurements, with a standard deviation of approximately ±3°.

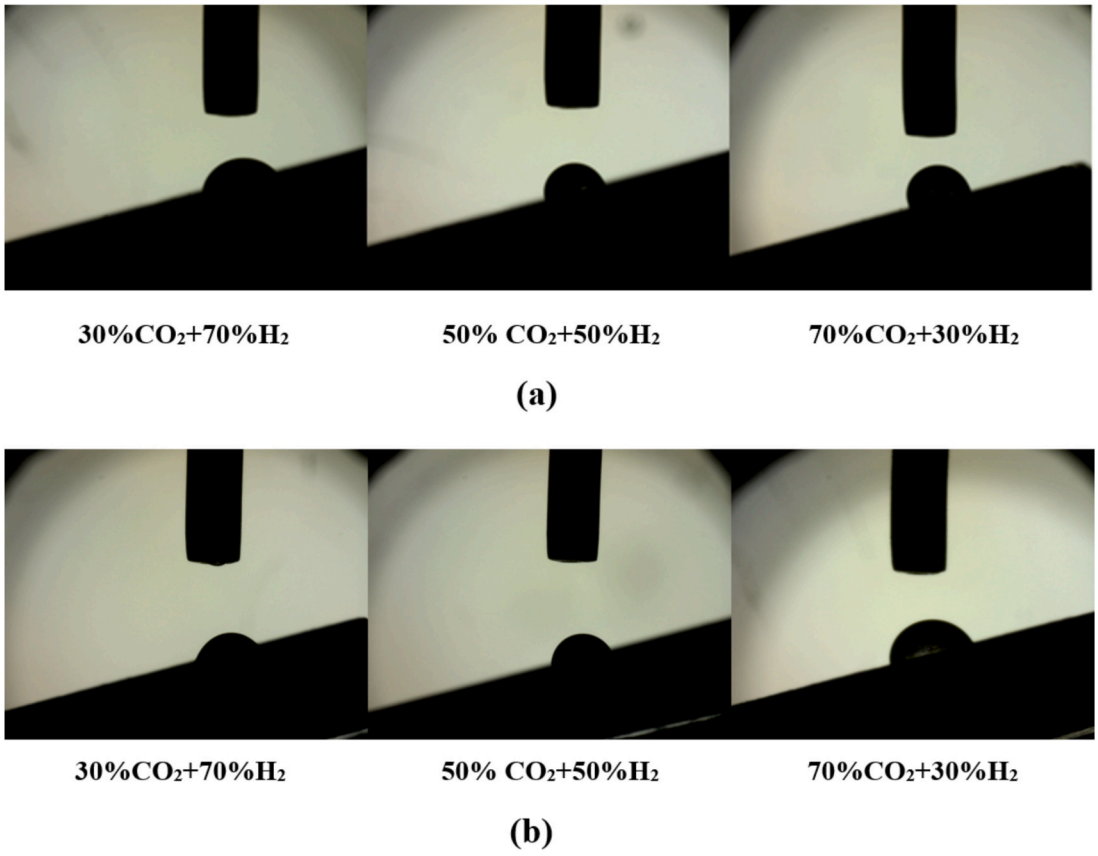

Fig. 9. Brine droplets on the carbonate rock substrate in the presence of a gas mixture of 30 % CO_2 + 70 % H_2, 50 % CO_2 + 50 % H_2, and 70 % CO_2 + 30 % H_2 at a pressure of 1200 psi and two temperatures of: a) $T = 50$ °C b) $T = 80$ °C.

2.4. Accuracy of the measurement

To verify the accuracy of the measurements, the contact angle in the systems of H_2/pure water/calcite at a temperature and pressure of 50 °C and 500 psi was measured and compared with the values reported in the literature. The Fig. 4 shows that the measured contact angle is about 40.5°, which is in agreement with the published data from [46,50,51].

2.5. Safety equipment

Given the highly flammable nature of hydrogen gas and the necessity of adhering to safety protocols while handling it, the use of appropriate safety equipment is crucial. Accordingly, considering the laboratory conditions for conducting tests, a gas detector was developed to identify potential leaks in the system, as shown in Fig. S2 in the supplementary material. The detector is based on an electrochemical sensor named MQ-8. This sensor has been calibrated according to the IEC-60079-29-1 standard, and it can be used as a portable device. It is also capable of measuring hydrogen gas concentrations in the range of 100 ppm to 10,000 ppm, but calibrated for a range of 100 ppm to 2000 ppm. The detector achieves maximum accuracy under standard environmental conditions, including a temperature of 25 °C and a humidity level of 65 %. The threshold for this device is set at 200 ppm.

3. Results and discussion

The wettability of a mineral surface is primarily influenced by its intrinsic surface properties, the types of fluids in contact with it, and the thermodynamic conditions of the system [52]. Therefore, it is essential to have a thorough comprehension of the various parameters that affect wettability for safe and cost-effective H_2 storage. In this regard, different mixtures of H_2/CO_2 at various ranges of pressure and temperature conditions were employed to investigate the wetting characteristic of the carbonate substrate used in this study. This section discusses how these factors control the wettability of the carbonate surface.

List the overall results of the contact angle values measured under various thermodynamic conditions used in this work (Table 1).

3.1. Effect of pressure

Fig. 5 shows the advancing and receding contact angles for the CO_2 + H_2/brine/carbonate system as a function of pressure. This involves three distinct CO_2 and H_2 combination ratios, at two temperatures of 50 °C and 80 °C. As shown in Fig. 5, the results suggest that an increase in pressure does not notably affect the wetting characteristics of the carbonate surface. For instance, at a constant temperature of 50 °C for the mixture of [30 % CO_2 + 70 % H_2] and [50 % CO_2 + 50 % H_2], and [70 % CO_2 + 30 % H_2], when the pressure increased from 500 to 3000 psi, the advancing and receding contact angles remained relatively unchanged and within the range of experimental error, at (54°, 49°), (76°, 71°), and (99°, 92°), respectively.

Some investigations into the wettability of carbonate rock for underground hydrogen storage have shown that an increase in pressure leads to an increased contact angle, implying a reduction in water wettability of the rock [46,53]. Some other studies, focused on the rock wettability in the presence of CO_2, have demonstrated that variations in pressure do not substantially alter wetting characteristics of the carbonate surface [29,54–57]. The results of this work also highlight that the contact angle remained unaffected as pressure changes, regardless of the composition of the gas. This similarity indicates that in our system, the effect of pressure on CO_2 is more dominant, mirroring the behavior of systems with pure CO_2.

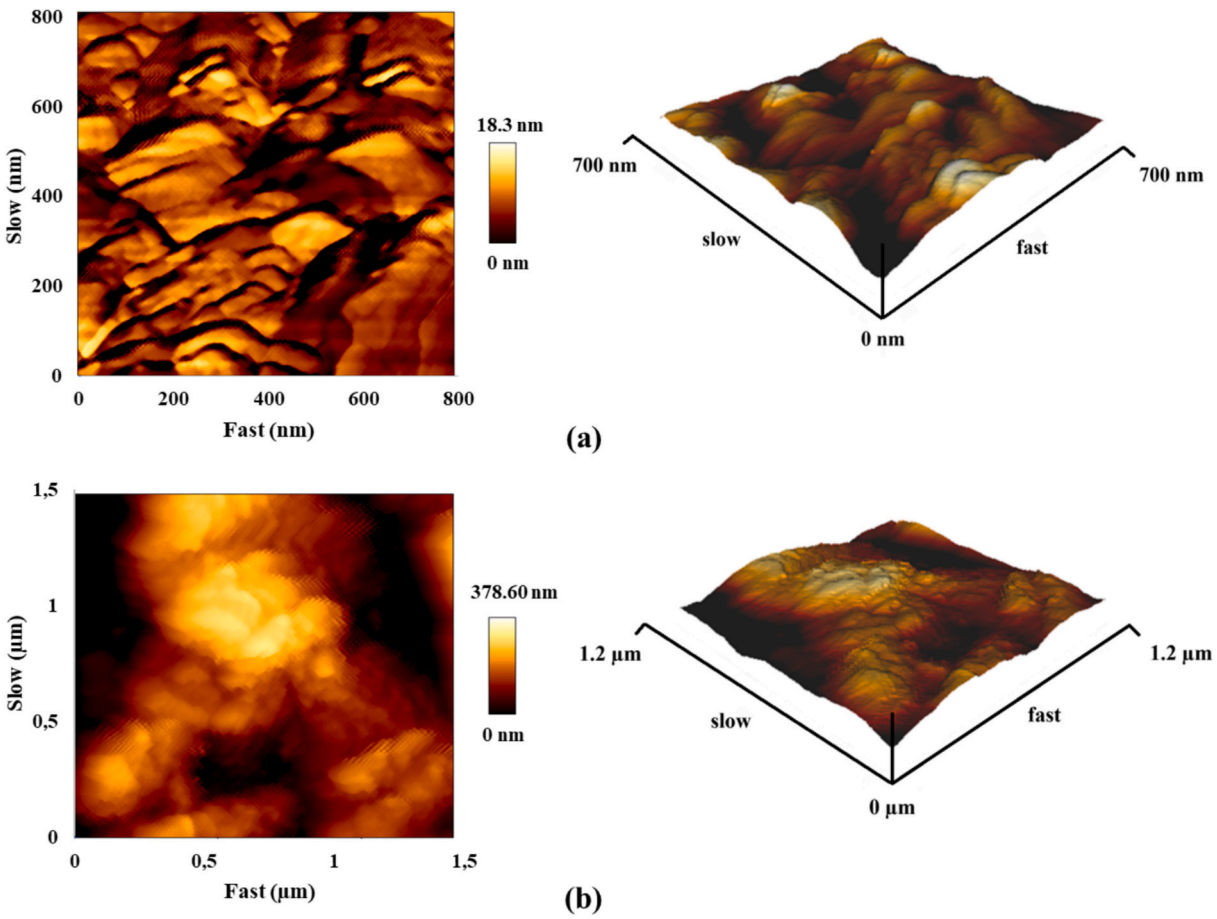

Fig. 10. 3D (right) and 2D (left) images obtained from the atomic force microscope (AFM) test related to the surface of carbonate substrates: a) before the test and b) after the test with a mixture of 30 % H_2 + 70 % CO_2.

Table 2
Statistical values derived from the AFM test.

Sample	R_a (nm)	R_q (nm)	R_{ti} (nm)
Carbonate – before test	56.89	68.12	353.33
Carbonate – after test	36.52	44.76	252.3

3.2. Effect of temperature

Fig. 6 shows the advancing and receding contact angles in the CO_2 + H_2/brine/carbonate system as a function of temperature under various CO_2 and H_2 combinations and at different pressures. For each isobar, increasing the temperature from 50 °C to 80 °C led to a reduction of contact angle, indicating a tendency of the rock to become more water-wet. For instance, at a constant pressure of 2000 psi for a mixture of [70 % CO_2 + 30 % H_2], when the temperature increased from 50 °C to 80 °C, the advancing and receding contact angles decreased from 103.6° to 80.5° and 47.9° to 33.5°, respectively.

The experimental findings from this study are in agreement with the broader observations in studies involving H_2 and CO_2, where an increase in temperature typically has been shown to enhance the wetting characteristic of the carbonate surface [26,46,53,57–61]. Zeng et al. utilized geochemical modeling to elucidate that when temperature increases, the disjoining pressure acting on the surface of calcite increases. This increased pressure enhances the repulsive effect of H_2 against calcite, resulting in the surface of carbonate exhibiting less wetness to H_2 as temperature increases [58]. Additionally, Bennion et al. discovered that the relative permeability of CO_2 increased with rising temperature in carbonate core samples at a constant water saturation. This suggested that as the temperature increased, the system shifted from being weakly CO_2-wet to becoming more water-wet [61].

Adding to the previously mentioned hypothesis, a reduction in contact angle due to temperature could be attributed to the decrease in the density of the gas mixture with increasing temperatures, as depicted in Fig. 7. The decreasing density could result in fewer interactions between the gas and the solid surface. This could, in turn, result in an increase in water wettability of the surface. Furthermore, the cohesive energy density of a gas mixture tends to decrease with increasing temperature due to the higher kinetic energy of gas molecules [26,62], whereas the cohesive energy density of the solid tends to remain relatively constant with temperature [63]. In this context, with rising temperature, the disparity in cohesive energy density between the solid (such as rock) and the gas mixture becomes more pronounced. This divergence in cohesive energy densities can result in less favorable interactions between the solid and gas molecules at higher temperatures, which promotes a shift toward more water-wetting of the surface.

3.3. Effect of CO_2 concentration

Fig. 8 shows advancing and receding contact angles for the CO_2 + H_2/brine/carbonate system as a function of CO_2 mole percentage for two temperatures (50 and 80 °C) and four pressures (500, 1200, 2000, and 3000 psi). Fig. 9 also depicts the profile of the brine droplets on the carbonate substrate, exposed to different combinations of H_2 and CO_2 at a pressure of 1200 psi and temperatures of 50 °C and 80 °C. The results indicate that by increasing the CO_2 concentration, the contact angle increases, and the rock becomes less water-wet. For instance, at a constant pressure of 1200 psi and temperature of 80 °C when the CO_2 mole

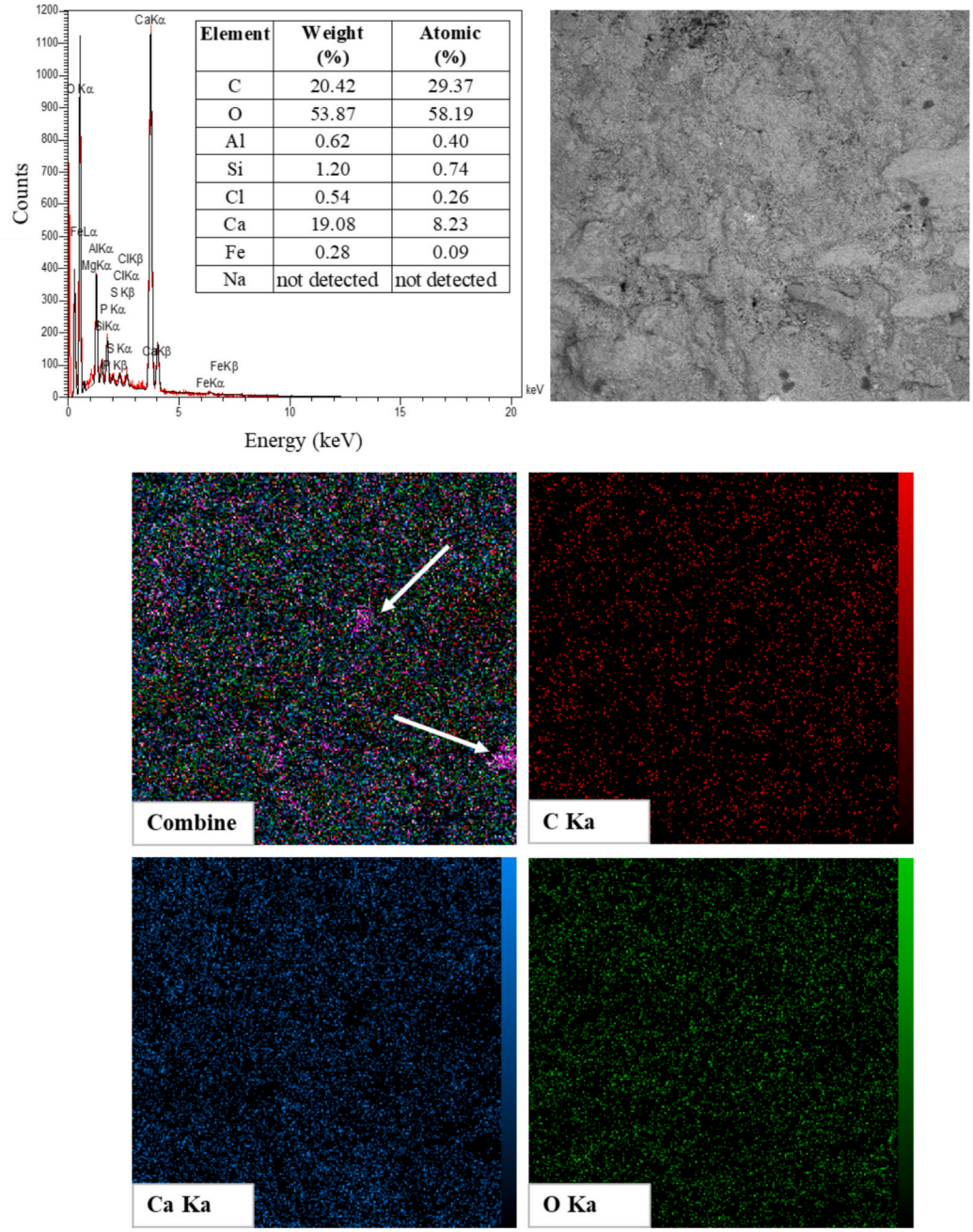

Fig. 11. The results of EDS tests and the elemental analysis map related to the carbonate sample before the contact angle test.

percent changes from 30 % to 70 %, the advancing and receding contact angles increased from 37.7° to 78.3° and 32.4° to 73.3°, respectively.

The system, including CO_2 tends to exhibit higher contact angle values compared to H_2 due to the higher density of CO_2 [6,31,65]. Consequently, when the CO_2 concentration in a gas mixture is increased, the overall density of the mixture also increases. For example, at a temperature of 50 °C and pressure of 2000 psi, by increasing the CO_2 content, the density of the mixture increased from 0.074 g/cm^3 to 0.209 g/cm^3. This heightened density increase leads to a substantial rise in the contact angle.

The results of the AFM tests for the analyzed samples before and after contact with the fluids (30 % H_2 + 70 % CO_2) and their statistical parameters are shown in Fig. 10 and Table 2, respectively. In these figures, the deepest valley is located at zero coordinates, and therefore, the height shown is obtained from the total depth of the deepest valleys with the highest peaks. The data from Table 2 indicates that exposure of the carbonate sample to a gas mixture containing CO_2 resulted in notable reductions in surface roughness parameters. Specifically, R_a decreased by 36 %, R_q by 34 %, and R_{ti} by 29 %. Such decreases in roughness parameters could potentially influence surface properties, including the surface wetting characteristic. In this regard, the dissolution of CO_2 in brine leads to a decrease in the solution's pH, typically reaching around 3.5, and forms a weak carbonic acid. The generated acid could dissolve some portions of the calcite minerals, resulting in a physically heterogeneous surface. This dissolution process has eventually resulted in a smoother surface and a reduction in surface roughness. Other researchers demonstrated that decreasing surface roughness leads to an increase in contact angles [26,66,67]. This phenomenon can be explained by Wenzel's equation [68], which describes how surface roughness affects wettability, as follows:

$$cos\theta_{rough} = rcos\theta_{smooth} \quad (1)$$

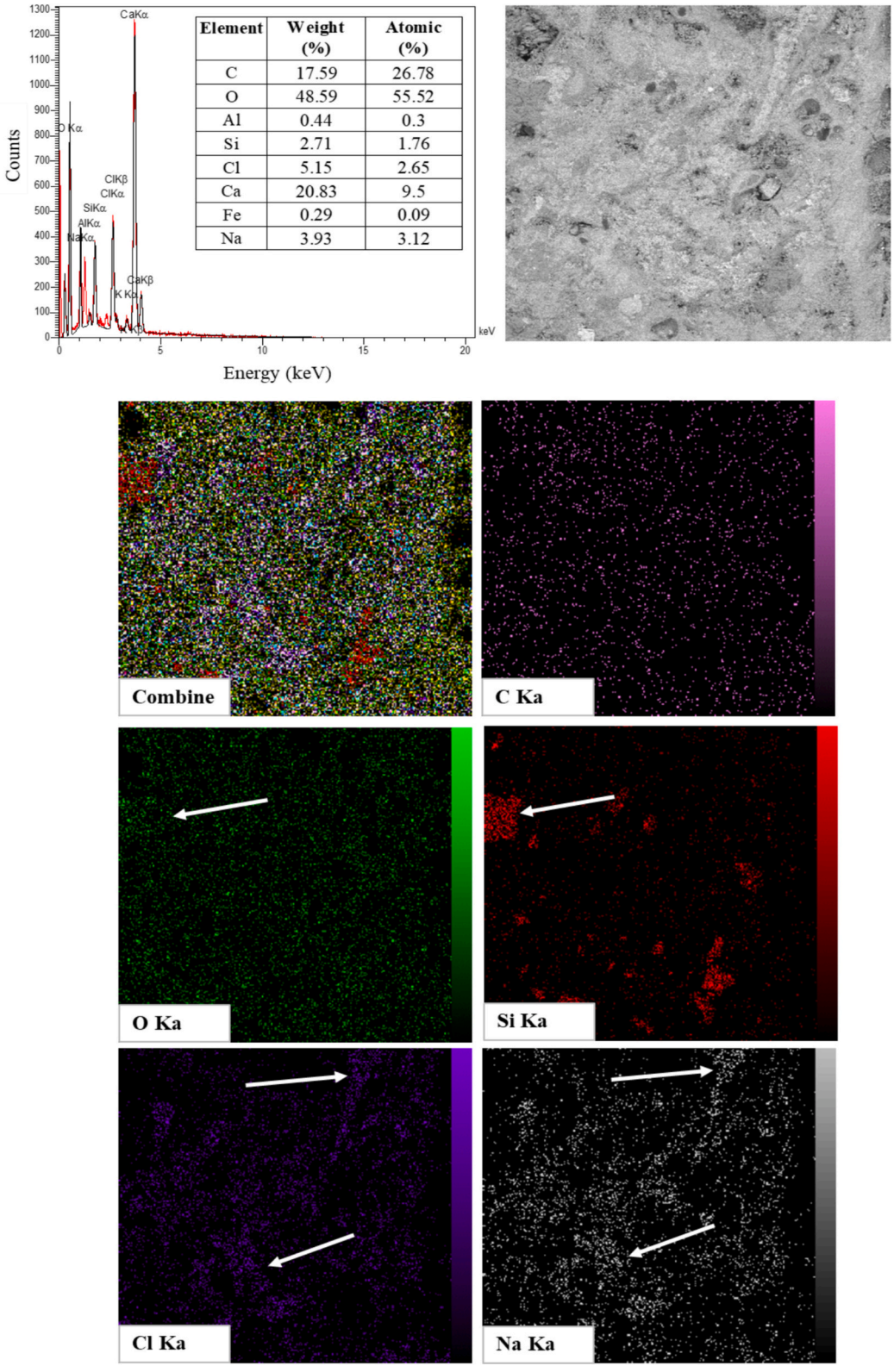

Fig. 12. The results of EDS tests and the elemental analysis map related to the carbonate sample after the contact angle test.

Where θ_{rough} is actual contact angle measured on the rough surface, θ_{smooth} is contact angle corresponding to the ideal smooth surface, and r is roughness ratio, which is defined as the ratio of the actual surface area to the projected smooth surface area and is always >1. Consequently, a decrease in surface roughness lowers the roughness ratio (r), which increases the apparent contact angle (reducing cos θ) and makes the surface less water-wet. According to this theory, a rough surface increases the solid–liquid contact area compared to a perfectly smooth surface, as the droplet fully wets the grooves. This enhanced contact leads to greater surface wetting and, consequently, a lower contact angle [69,70].

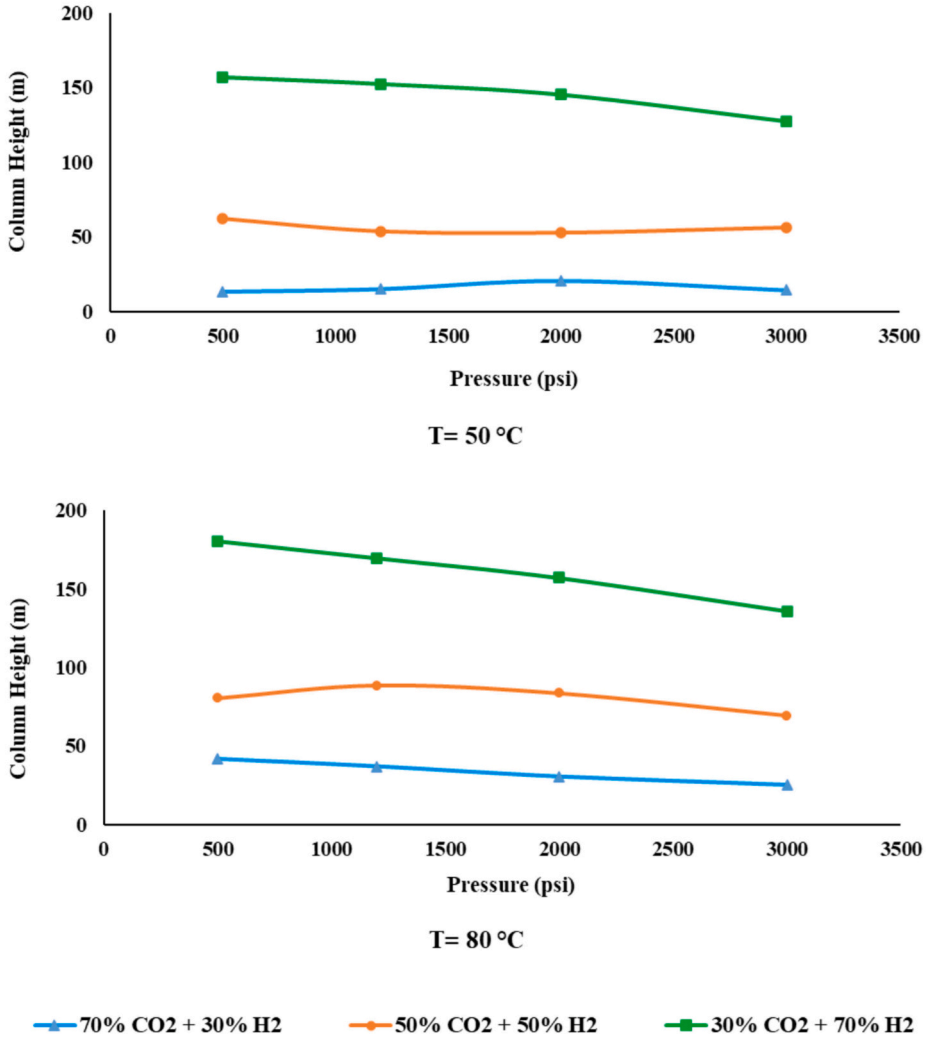

Fig. 13. Maximum gas column height as a function of pressure for two temperatures of 50 °C and 80 °C.

Therefore, increasing the mole fraction of CO_2 results in greater dissolution of the rock sample, reduced roughness, and higher contact angles in carbonate rocks. It is worth noting that CO_2 does not consistently impact surface roughness and wettability. Unlike carbonate rocks, AFM tests have shown no notable change in the Root Mean Square (RMS) roughness of sandstone after exposure to CO_2 under identical conditions. This indicates that the surface of sandstone remains unaffected by carbonic acid, which forms when CO_2 dissolves in brine. As a result, sandstone retains its original roughness and, consequently, its wettability remains unchanged [33].

The results of EDS tests for the carbonate sample, before and after exposure to the mixture of 30 % H_2 + 70 % CO_2, are illustrated in Fig. 11 and Fig. 12, respectively. In Fig. 11, it is evident that the primary components in the samples are carbon, oxygen, and calcium, the key elements of calcium carbonate. Consequently, the predominant compound in the analyzed samples is identified as $CaCO_3$. Apart from these elements, the sample contains additional elements like magnesium, silica, aluminum, iron, chlorine, sulfur, and phosphorus. The distribution of carbon, oxygen, and calcium is uniform across the material, but there is a localized accumulation of silicon and aluminum in specific regions (highlighted by white arrows). This suggests the presence of aluminum silicate as an impurity compound in the samples. On the other hand, Fig. 12, depicting the carbonate sample after the test, reveals carbon, calcium, and oxygen as the predominant elements in the structure, too. Interestingly, there is an evident increase in the values of silicon (Si), chlorine (Cl), and sodium (Na) elements compared to the pre-test sample. The accumulation of sodium in regions where chlorine is concentrated suggests the presence of deposited salt crystals in those areas (highlighted by white arrows). The precipitation of these salt crystals, used in the brine, suggests the dissolution of carbonate rock by the weak carbonic acid mentioned before. In addition, in regions with higher silicon content, the presence of oxygen suggests the existence of SiO_2 in those specific areas (highlighted by white arrows). It appears that the increased percentage of insoluble phases, like quartz, in the system is attributed to the partial dissolution of the carbonate rock. Consequently, elemental analysis revealed that after exposure to CO_2 gas, there was a change in the carbonate's elemental concentration, indicating a chemical reaction.

4. Implication

In underground hydrogen storage within porous formations, one of the critical factors is the maximum height of stored hydrogen beneath the caprock, impacting structural trapping. Surpassing this height allows hydrogen to permeate the caprock by overcoming its capillary pressure [71]. To be more specific, structural trapping is a crucial requirement and the most significant mechanism for containing the highly buoyant gas within a geological formation [72]. Because hydrogen is much less dense than formation water and migrates upward due to gravity, a subsurface structural trap with tight, impermeable seal rocks is needed

Table 3
Maximum gas column height and required parameters for its calculation at different conditions [64,77].

Gas mixture (mole%)	Pressure (psi)	Temperature (°C)	Average θ (°)	IFT (mN/m)	Δρ (g/cm3)	MGCH (m)
70 % CO_2 + 30 % H_2	500	50	93.55	54.77	0.987	13.54
	500	80	77.45	47.75	0.978	41.81
	1200	50	95.25	38.73	0.918	15.21
	1200	80	75.8	35.26	0.920	37.06
	2000	50	97.05	34.87	0.826	20.43
	2000	80	78.1	31.89	0.846	30.62
	3000	50	94.65	32.14	0.710	14.47
	3000	80	80.6	29.56	0.754	25.25
50 % CO_2 + 50 % H_2	500	50	74.85	60.62	1.000	62.44
	500	80	66.95	51.47	0.989	80.28
	1200	50	74.85	49.93	0.957	53.74
	1200	80	61.5	44.78	0.952	88.51
	2000	50	73.5	42.76	0.906	52.82
	2000	80	59.7	38.1	0.908	83.48
	3000	50	71.6	38.24	0.845	56.32
	3000	80	64.8	35.28	0.855	69.28
30 % CO_2 + 70 % H_2	500	50	52.05	65.45	1.012	156.82
	500	80	38.9	58.91	1.000	180.74
	1200	50	49.85	59.19	0.987	152.36
	1200	80	35.05	51.48	0.978	169.85
	2000	50	50.5	55.64	0.960	145.27
	2000	80	36.15	47.13	0.954	157.26
	3000	50	54.5	51.71	0.928	127.49
	3000	80	42.1	43.04	0.925	136.03

above the reservoir to prevent leakage [73]. The storage capacity of seal rock, which quantifies the amount of hydrogen that can be accumulated in porous rock beneath it, is typically defined as the Maximum Hydrogen Column Height (MHCH). This height is derived from the force balance over the entire gas column, considering buoyancy, gravity, and capillary forces during underground H_2 storage: Buoyancy force - Gravity force = Capillary force. Consequently, using this equation, the gas column height that can be permanently immobilized beneath the caprock can be estimated, and assessing this height is vital to avoid capillary breakthroughs into the caprock [71,74]. In this context, Berg [75] has analytically assessed the relative capillary contributions from both seal and reservoir rocks to balance hydrocarbon buoyancy in petroleum systems [75]. This approach could be used for Underground Hydrogen Storage (UHS) too, since Thanasaksukthawee et al. [76] showed that the contribution from reservoir characteristics, such as pore size, is a significant factor when analyzing gas storage potential through column height estimation [76]. Therefore, the maximum gas column height in UHS, including hydrogen and cushion gas, can be expressed as:

$$h_{max} = \frac{2\sigma\cos\theta}{\Delta\rho g}\left(\frac{1}{R_{seal}} - \frac{1}{R_{res}}\right) \quad (1)$$

where R_{seal} and R_{res} are the radius of the narrowest pore throat of seal rock and reservoir rock, respectively, σ is the interfacial tension (IFT), θ is the gas-water contact angle, g is the gravitational constant, $\Delta\rho$ is the density difference between water and gas, and h_{max} is the maximum gas column height, including hydrogen and cushion gas [75]. To calculate the column height of the gas mixture, the interfacial tension between H_2 + CO_2 and brine and the density difference between them were extracted from [64,77], respectively. In this regard, the results from Isfehani et al. [77] suggest that when both pressure and temperature are increased, there is a corresponding decrease in the IFT between brine and a gas mixture composed of CO_2 and H_2. The gravitational constant was also set to 9.81 (m/s^2). Since direct measurement of the limiting pore and throat radius is not feasible, a common approach is to estimate the pore throat radius using a porosity-permeability relationship [75,78]. For example, an effective grain size (D_e) can be calculated from core analysis using an empirical permeability equation such as:

$$D_e = \left(1.89kn^{-5.1}\right)^{0.5} \quad (2)$$

where k is the permeability (mD) and n is the porosity (percent) [75]. The throat sizes (r_t) can then be estimated using D_e and assuming a theoretical packing geometry using Eq. (3) [79].

$$r_t = 0.5 \times 0.154\, D_e \quad (3)$$

According to Eqs. (2) and (3), our estimated pore throat radius of reservoir rock (R_{res}) is 1.5 μm. The capillary force is inversely related to the pore radius (R_{seal}) of the caprock. As a result, a tight caprock exerts a stronger capillary force against the buoyancy force of the hydrogen column in a storage site. Shale, commonly used as a seal in geological formations, typically has pore sizes between 5 nm and 100 nm [80]. Hence, a pore radius of 50 nm is used as a standard value for the caprock, supported by other research [71,81]. Furthermore, it is important to mention that in Eq. (1), θ is the CO_2 + H_2/brine/seal rock contact angle, which quantifies the caprock's wettability. As a result, using the reservoir rock's contact angle instead of it might provide a conservative estimate because shale, a common cap rock, is more wetting to the gas than the reservoir rock. Specifically, shale rocks, being richer in clay and organic matter, tend to be more hydrophobic and often have higher contact angles. This means that the cap rock would offer better sealing than estimated in this section, resulting in a more secure trap for the gas column.

Fig. 13 illustrates the effect of pressure, temperature, and gas composition on the maximum column height of the gas mixture in the carbonate rock under study, with detailed data available in Table 3. A notable reduction in the maximum height of the gas column occurs with an increase in the fraction of CO_2 as the cushion gas. For instance, under conditions of $P = 1200$ psi and $T = 50$ °C, the column height of the gas mixture decreased from 152.36 m to 15.21 m when the CO_2 mole percentage increased from 30 % to 70 %. The decrease in both IFT and $\cos\theta$ with an increase in the mole fraction of CO_2 outweighs the minor decrease in density difference between the gas mixture and brine, which leads to a reduction in the gas column height. In addition, as shown in Fig. 13, the maximum column height for any combination of CO_2 and H_2 increases with an increase in temperature. For instance, at a pressure of 1200 psi, the column height of the gas mixture (50 % CO_2 + 50 % H_2) increased from 53.74 m to 88.51 m by increasing the temperature from 50° to 80°. The change in IFT between the gas mixture and brine, as well as the density difference with temperature, is not significant compared to the variation of contact angle with temperature. This results in the dominant effect of the rock wettability on the gas column height, which means that decreasing the contact angle with temperature leads to an increase in the gas column height. Furthermore, Fig. 13 indicates that increasing pressure causes a decrease in the gas column height for the 30 % CO_2 + 70 % H_2 mixture, whereas there is no significant alteration in the gas column height for the other two mixtures with a higher CO_2 fraction. In this regard, the result of this study indicates that the contact angle remains relatively constant under varying pressures for different combinations of CO_2 and H_2. Moreover, increasing the pressure results in a reduction of IFT and density difference between the mixture of CO_2 and H_2 and brine [64,77]. Consequently, the variation in IFT and density difference with pressure counterbalance each other's impact, yielding insignificant alteration in gas column height as pressure changes. However, in mixtures with a higher fraction of H_2, the reduction of the density difference between the gas mixture and brine by pressure becomes less notable, causing the decrease in the maximum height of the gas column with increasing pressure to directly correlate with the reduction in IFT. For instance, for a mixture of 30 % CO_2 + 70 % H_2, the gas column decreased from 156.82 m to 127.49 m when pressure increased from 500 psi to 3000 psi at a temperature of 50°, whereas the column height of the gas mixture (70 % CO_2 + 30 % H_2) for pressures of

500 psi and 3000 psi is 13.54 and 14.47 m, respectively.

Thus, understanding the wettability state of calcite is vital for assessing H_2 geo-storage capacity in carbonate formations, given that calcite is prevalent in both caprock and reservoir rock [82,83]. This characterization is particularly crucial as it significantly impacts structural trapping (in the presence of a calcite-rich caprock) and residual trapping (in the case of a calcite-rich reservoir rock) [84–86]. In this study, a water-wet state was identified under reservoir conditions (high pressure and high temperature) when the gas mixture contained 50 % or less CO_2. In water-wet conditions within the host rock, gas tends to occupy larger pores, which results in an increased gas column height and, consequently, a greater hydrogen storage capacity, as the hydrogen column height is directly correlated with storage capacity [47,87]. However, pore-scale modelling indicates that in water-wet conditions, during hydrogen injection (drainage), the snap-off effect occurs at pore throats where water films can reconnect, breaking the continuous hydrogen phase into disconnected bubbles. This fragmentation prevents hydrogen from accessing all available pore spaces, which reduces storage efficiency [88].

Moreover, as shown in Table 3, in the presence of a gas mixture with a high percentage of CO_2 (70 % CO_2 + 30 % H_2), the carbonate rock tends to become more gas-wet, which may contribute to a reduction in calculated gas column height. During the primary imbibition process (hydrogen extraction), increased hydrogen wetting leads to larger and more stable hydrogen clusters, which hinders efficient extraction. In contrast, during primary forced imbibition, reducing water-wet conditions can enhance hydrogen recovery by preventing snap-off. Specifically, in strongly water-wet rocks, hydrogen clusters break into smaller, dispersed clusters during forced imbibition, resulting in ineffective extraction. This dispersed state increases residual hydrogen saturation, making it difficult to withdraw hydrogen efficiently during periods of high energy demand due to phase disconnection and trapping [88–90].

Additionally, it is worth noting that injecting a high percentage of CO_2 into carbonate reservoirs as cushion gas for hydrogen storage may present an additional challenge, which is potential interactions between CO_2 and carbonates [16]. This process leads to carbonate dissolution, affecting the overall integrity of the reservoir. Specifically, the dissolution of calcite could compromise caprock stability and long-term sealing capacity. Hence, these findings highlight the complex trade-offs associated with using different concentrations of CO_2 as cushion gas. That is, at lower CO_2 concentrations, while larger gas column height can be acheived, more water-wet state of the carbonate rock tends to create less favorable conditions for hydrogen recovery, due to stronger snap-off effect by water and higher trapped hydrogen volume [91,92]. In contrast, higher concentrations of CO_2 appear to make the carbonate rock more intermediate-wet, which despite reducing the maximum gas column height limit, mitigates the snap-off effect and enhances the hydrogen recovery. Therefore, managing the wettability of the storage formation by injecting an optimized fraction of CO_2 as cushion gas could play a key role in optimizing hydrogen injection and recovery and enhancing storage capacity.

5. Conclusions

In Underground Hydrogen Storage (UHS), the use of cushion gas is crucial for enabling hydrogen extraction by providing the necessary pressure. The distribution and entrapment of hydrogen are governed by the system's wettability, affecting flow rates, storage capacity, and containment security. This study investigates carbon dioxide as a cushion gas in carbonate systems, using the tilted plate method to assess rock wettability under varying pressure, temperature, and CO_2 concentrations. Key findings are summarized below:

- Pressure variations had minimal effect on carbonate wettability across the tested temperature and CO_2 concentration scenarios.
- Increasing temperature (50 °C to 80 °C) reduced the contact angle, indicating a shift toward more water-wet behavior.
- Increasing CO_2 concentration (30 % to 70 %) shifted the wettability from more water-wet to intermediate-wet. AFM and EDS analyses revealed a decrease in surface roughness and dissolution due to carbonic acid, explaining the wettability shift.
- Maximum storage column heights increased with temperature but decreased with rising CO_2 concentration. Pressure reduced column height at 30 % CO_2, but this effect was less significant at higher CO_2 levels.
- The calculated gas column height shows that a water-wet state with $\leq$50% CO_2 may enhance hydrogen storage capacity, but stronger snap-off effect, under such conditions, would reduce hydrogen recovery efficiency. Thus, regulating CO_2 levels as a cushion gas is crucial for optimizing storage performance.

CRediT authorship contribution statement

Amirmansour Jafari: Writing – original draft, Formal analysis, Data curation, Conceptualization. **Zoha Dalal Isfehani:** Writing – original draft, Visualization, Validation, Formal analysis, Conceptualization. **Jalal Fahimpour:** Writing – review & editing, Validation, Supervision, Project administration, Methodology, Investigation, Funding acquisition, Formal analysis, Conceptualization. **Nima Shokri:** Writing – review & editing, Validation. **Mirhasan Hosseini:** Writing – review & editing, Validation, Formal analysis. **Mohammad Sharifi:** Writing – review & editing, Supervision, Resources, Funding acquisition.

Declaration of competing interest

The authors declare that they have no known competing financial interests or personal relationships that could have appeared to influence the work reported in this paper.

Appendix A. Supplementary data

Supplementary data to this article can be found online at https://doi.org/10.1016/j.est.2025.117274.

Data availability

Data will be made available on request.

References

[1] E.R. Okoroafor, S.D. Saltzer, A.R. Kovscek, Toward underground hydrogen storage in porous media: reservoir engineering insights, Int. J. Hydrog. Energy 47 (79) (2022) 33781–33802.
[2] H. Song, et al., A novel hybrid energy system for hydrogen production and storage in a depleted oil reservoir, Int. J. Hydrog. Energy 46 (34) (2021) 18020–18031.
[3] A.M. Elberry, et al., Large-scale compressed hydrogen storage as part of renewable electricity storage systems, Int. J. Hydrog. Energy 46 (29) (2021) 15671–15690.
[4] H. Hematpur, et al., Review of underground hydrogen storage: concepts and challenges, Adv. Geo-Energ. Res. 7 (2) (2023) 111–131.
[5] J. Miocic, et al., Underground hydrogen storage: a review, Geol. Soc. Lond. Spec. Publ. 528 (1) (2023) (p. SP528-2022-88).
[6] S. Iglauer, M. Ali, A. Keshavarz, Hydrogen wettability of sandstone reservoirs: implications for hydrogen geo-storage, Geophys. Res. Lett. 48 (3) (2021) e2020GL090814.
[7] M. Berta, et al., Geochemical effects of millimolar hydrogen concentrations in groundwater: an experimental study in the context of subsurface hydrogen storage, Environ. Sci. Technol. 52 (8) (2018) 4937–4949.
[8] N. Heinemann, et al., Hydrogen storage in saline aquifers: the role of cushion gas for injection and production, Int. J. Hydrog. Energy 46 (79) (2021) 39284–39296.
[9] J. Mouli-Castillo, N. Heinemann, K. Edlmann, Mapping geological hydrogen storage capacity and regional heating demands: an applied UK case study, Appl. Energy 283 (2021) 116348.
[10] M. Panfilov, Underground and pipeline hydrogen storage, in: Compendium of hydrogen energy, Elsevier, 2016, pp. 91–115.
[11] M. Saeed, P. Jadhawar, Optimizing underground hydrogen storage in aquifers: the impact of cushion gas type, Int. J. Hydrog. Energy 52 (2024) 1537–1549.

[12] A. Jahanbakhsh, et al., Underground hydrogen storage: a UK perspective, Renew. Sust. Energ. Rev. 189 (2024) 114001.
[13] D.S. Mahdi, et al., Hydrogen Underground Storage Efficiency in a Heterogeneous Sandstone Reservoir, 2021.
[14] F. Alnili, et al., Carbon dioxide/brine wettability of porous sandstone versus solid quartz: an experimental and theoretical investigation, J. Colloid Interface Sci. 524 (2018) 188–194.
[15] E.A. Al-Khdheeawi, et al., Impact of reservoir wettability and heterogeneity on CO2-plume migration and trapping capacity, Int. J. Greenh. Gas Contr. 58 (2017) 142–158.
[16] S. Prigmore, et al., Cushion gas consideration for underground hydrogen storage, Encyclopedia 4 (2) (2024) 847–863.
[17] N. Heinemann, et al., Enabling large-scale hydrogen storage in porous media–the scientific challenges, Energy Environ. Sci. 14 (2) (2021) 853–864.
[18] J. Laille, J. Molinard, A. Wents, Inert gas injection as part of the cushion of the underground storage of Saint-Clair-Sur-Epte, France, in: SPE Unconventional Resources Conference/Gas Technology Symposium, SPE, 1988.
[19] M. Dussaud, M. Tek, Underground Storage of Natural Gas, Springer Netherlands, Dordrecht, 1989.
[20] C.M. Oldenburg, Carbon dioxide as cushion gas for natural gas storage, Energy Fuel 17 (1) (2003) 240–246.
[21] W.T. Pfeiffer, S. Bauer, Subsurface porous media hydrogen storage–scenario development and simulation, Energy Procedia 76 (2015) 565–572.
[22] V. Mirchi, M. Dejam, V. Alvarado, Interfacial tension and contact angle measurements for hydrogen-methane mixtures/brine/oil-wet rocks at reservoir conditions, Int. J. Hydrog. Energy 47 (82) (2022) 34963–34975.
[23] R. Farokhpoor, et al., CO2 wettability behavior during CO2 sequestration in saline aquifer-an experimental study on minerals representing sandstone and carbonate, Energy Procedia 37 (2013) 5339–5351.
[24] J. Wang, et al., Analysis of the impact of CO2 adsorption on rock wettability for geological storage of CO2, Energy Fuel 37 (18) (2023) 14046–14052.
[25] S.I. Eyitayo, et al., Experimental investigation of the impact of CO2 injection strategies on rock wettability alteration for CCS applications, Energies 17 (11) (2024) 2600.
[26] M. Arif, et al., CO2 storage in carbonates: wettability of calcite, Int. J. Greenh. Gas Contr. 62 (2017) 113–121.
[27] A. Al-Yaseri, et al., Rock-wettability impact on CO2-carbonate rock interaction and the attendant effects on CO2Storage in carbonate reservoirs, J. Nat. Gas Sci. Eng. 104 (2022) 104664.
[28] C. Garing, S. Benson, CO2 wettability of sandstones: addressing conflicting capillary behaviors, Geophys. Res. Lett. 46 (2) (2019) 776–782.
[29] R. Farokhpoor, et al., Wettability behaviour of CO2 at storage conditions, Int. J. Greenh. Gas Contr. 12 (2013) 18–25.
[30] A. Ali, D.R. Cole, A. Striolo, Cushion gas effects on clay-hydrogen-brine wettability at conditions relevant to underground gas storage, Int. J. Hydrog. Energy 58 (2024) 668–677.
[31] M. Ali, et al., Influence of pressure, temperature and organic surface concentration on hydrogen wettability of caprock; implications for hydrogen geo-storage, Energy Rep. 7 (2021) 5988–5996.
[32] L. Hashemi, et al., Contact angle measurement for hydrogen/brine/sandstone system using captive-bubble method relevant for underground hydrogen storage, Adv. Water Resour. 154 (2021) 103964.
[33] Z.D. Isfehani, et al., Sandstone wettability and mixed gas composition: unraveling the impact of CO2 in hydrogen geo-storage, Int. J. Hydrog. Energy 59 (2024) 1352–1366.
[34] N.S. Muhammed, B. Haq, D. Al Shehri, Role of methane as a cushion gas for hydrogen storage in depleted gas reservoirs, Int. J. Hydrog. Energy 48 (76) (2023) 29663–29681.
[35] N.S. Muhammed, B. Haq, D.A. Al Shehri, Hydrogen storage in depleted gas reservoirs using nitrogen cushion gas: a contact angle and surface tension study, Int. J. Hydrog. Energy 48 (98) (2023) 38782–38807.
[36] N.S. Muhammed, B. Haq, D. Al Shehri, CO2 rich cushion gas for hydrogen storage in depleted gas reservoirs: insight on contact angle and surface tension, Int. J. Hydrog. Energy 50 (2024) 1281–1301.
[37] A. Phan, et al., Simulation insights into wetting properties of hydrogen-brine-clay for hydrogen geo-storage, J. Energy Storage 112 (2025) 115477.
[38] X. Yu, et al., In-situ wettability alteration of organic-rich shale caprock in hydrogen with cushion gas: implications for hydrogen geo-storage, Int. J. Hydrog. Energy 103 (2025) 75–86.
[39] N. Liu, et al., Pore-scale study of microbial hydrogen consumption and wettability alteration during underground hydrogen storage, Front. Energy Res. 11 (2023) 1124621.
[40] H. Song, et al., A pore-scale simulation of the effect of heterogeneity on underground hydrogen storage, Water 16 (22) (2024) 3264.
[41] Q. Zhao, et al., Using X-ray computed tomography and pore-scale numerical modeling to study the role of heterogeneous rock surface wettability on hydrogen-brine two-phase flow in underground hydrogen storage, Fuel 366 (2024) 131414.
[42] R. Dehury, S. Chowdhury, J.S. Sangwai, Dynamics of hydrogen storage in subsurface saline aquifers: a computational and experimental pore-scale displacement study, Int. J. Hydrog. Energy 69 (2024) 817–836.
[43] Y. Wang, et al., Pore-scale simulation of H2-brine system relevant for underground hydrogen storage: a lattice Boltzmann investigation, Adv. Water Resour. 190 (2024) 104756.
[44] M. Arif, S.A. Abu-Khamsin, S. Iglauer, Wettability of rock/CO2/brine and rock/oil/CO2-enriched-brine systems: critical parametric analysis and future outlook, Adv. Colloid Interf. Sci. 268 (2019) 91–113.
[45] E. Gadelmawla, et al., Roughness parameters, J. Mater. Process. Technol. 123 (1) (2002) 133–145.
[46] M. Hosseini, et al., Hydrogen wettability of carbonate formations: implications for hydrogen geo-storage, J. Colloid Interface Sci. 614 (2022) 256–266.
[47] M. Hosseini, et al., Basalt-H2-brine wettability at geo-storage conditions: implication for hydrogen storage in basaltic formations, J. Energy Storage 52 (2022) 104745.
[48] R. Sedev, et al., Contact angles of a brine on a bituminous coal in compressed hydrogen, Geophys. Res. Lett. 49 (8) (2022) e2022GL098261.
[49] M. Hosseini, et al., Capillary sealing efficiency analysis of caprocks: implication for hydrogen geological storage, Energy Fuel 36 (7) (2022) 4065–4075.
[50] H. Esfandyari, et al., Experimental evaluation of rock mineralogy on hydrogen-wettability: implications for hydrogen geo-storage, J. Energy Storage 52 (2022) 104866.
[51] A. Safari, et al., Computational fluid dynamics modeling of rock–liquid–H2 contact angles: implications for underground hydrogen storage, J. Energy Storage 81 (2024) 110475.
[52] N. Yekeen, et al., Wettability of rock/CO2/brine systems: a critical review of influencing parameters and recent advances, J. Ind. Eng. Chem. 88 (2020) 1–28.
[53] J. Hou, et al., Salinity, temperature and pressure effect on hydrogen wettability of carbonate rocks, Int. J. Hydrog. Energy 48 (30) (2023) 11303–11311.
[54] P.K. Bikkina, Contact angle measurements of CO2–water–quartz/calcite systems in the perspective of carbon sequestration, Int. J. Greenh. Gas Contr. 5 (5) (2011) 1259–1271.
[55] D.N. Espinoza, J.C. Santamarina, Water-CO2-mineral systems: interfacial tension, contact angle, and diffusion—implications to CO2 geological storage, Water Resour. Res. 46 (7) (2010).
[56] S. Wang, I.M. Edwards, A.F. Clarens, Wettability phenomena at the CO2–brine–mineral interface: implications for geologic carbon sequestration, Environ. Sci. Technol. 47 (1) (2013) 234–241.
[57] N. Tonnet, D. Broseta, G. Mouronval, Evaluation of the petrophysical properties of a carbonate-rich caprock for CO2 geological storage purposes, in: SPE Europec Featured at EAGE Conference and Exhibition?, SPE, 2010.
[58] L. Zeng, et al., Hydrogen wettability in carbonate reservoirs: implication for underground hydrogen storage from geochemical perspective, Int. J. Hydrog. Energy 47 (60) (2022) 25357–25366.
[59] D. Broseta, N. Tonnet, V. Shah, Are rocks still water-wet in the presence of dense CO2 or H2S? Geofluids 12 (4) (2012) 280–294.
[60] D. Yang, Y. Gu, P. Tontiwachwuthikul, Wettability determination of the reservoir brine− reservoir rock system with dissolution of CO2 at high pressures and elevated temperatures, Energy Fuel 22 (1) (2008) 504–509.
[61] B. Bennion, S. Bachu, Relative permeability characteristics for supercritical CO2 displacing water in a variety of potential sequestration zones in the western Canada sedimentary basin, in: SPE Annual Technical Conference and Exhibition?, SPE, 2005.
[62] A.F. Barton, CRC handbook of solubility parameters and other cohesion parameters, Routledge, 2017.
[63] C. Kittel, P. McEuen, Introduction to Solid State Physics, John Wiley & Sons, 2018.
[64] A. Hassanpouryouzband, et al., Thermodynamic and transport properties of hydrogen containing streams, Sci. Data 7 (1) (2020) 222.
[65] A. Al-Yaseri, N.K. Jha, On hydrogen wettability of basaltic rock, J. Pet. Sci. Eng. 200 (2021) 108387.
[66] X. Liu, et al., Main factors controlling the wettability of gas shales: a case study of over-mature marine shale in the Longmaxi Formation, J. Nat. Gas Sci. Eng. 56 (2018) 18–28.
[67] A.Z. Al-Yaseri, et al., Receding and advancing (CO2+ brine+ quartz) contact angles as a function of pressure, temperature, surface roughness, salt type and salinity, J. Chem. Thermodyn. 93 (2016) 416–423.
[68] R.N. Wenzel, Resistance of solid surfaces to wetting by water, Ind. Eng. Chem. 28 (8) (1936) 988–994.
[69] G. Whyman, E. Bormashenko, T. Stein, The rigorous derivation of Young, Cassie–Baxter and Wenzel equations and the analysis of the contact angle hysteresis phenomenon, Chem. Phys. Lett. 450 (4–6) (2008) 355–359.
[70] P.S. Swain, R. Lipowsky, Contact angles on heterogeneous surfaces: a new look at Cassie's and Wenzel's laws, Langmuir 14 (23) (1998) 6772–6780.
[71] S. Iglauer, Optimum geological storage depths for structural H2 geo-storage, J. Pet. Sci. Eng. 212 (2022) 109498.
[72] S. Benson, Underground geological storage, IPCC Spec. Rep. Carbon Captur. Stor. (2005) 195–276.
[73] S.A. Rackley, Carbon capture and storage, Butterworth-Heinemann, 2017.
[74] M. Ghaedi, P.Ø. Andersen, R. Gholami, Maximum column height and optimum storage depth for geological storage of hydrogen, Int. J. Hydrog. Energy 50 (2024) 291–304.
[75] R.R. Berg, Capillary pressures in stratigraphic traps, AAPG Bull. 59 (6) (1975) 939–956.
[76] V. Thanasaksukthawee, et al., Relative CO2 column height for CO2 geological storage: a non-negligible contribution from reservoir rock characteristics, Energy Fuel 36 (7) (2022) 3727–3736.
[77] Z.D. Isfehani, et al., Interfacial tensions of (brine+ H_2+ CO_2) systems at gas geo-storage conditions, J. Mol. Liq. 374 (2023) 121279.
[78] M. Rezaee, A. Jafari, E. Kazemzadeh, Relationships between permeability, porosity and pore throat size in carbonate rocks using regression analysis and neural networks, J. Geophys. Eng. 3 (4) (2006) 370–376.
[79] M. Naylor, M. Wilkinson, R. Haszeldine, Calculation of CO2 column heights in depleted gas fields from known pre-production gas column heights, Mar. Pet. Geol. 28 (5) (2011) 1083–1093.

[80] D.N. Espinoza, J.C. Santamarina, CO2 breakthrough—Caprock sealing efficiency and integrity for carbon geological storage, Int. J. Greenh. Gas Contr. 66 (2017) 218–229.
[81] S. Iglauer, Optimum storage depths for structural CO2 trapping, Int. J. Greenh. Gas Contr. 77 (2018) 82–87.
[82] N. Tonnet, et al., Petrophysical assessment of a carbonate-rich caprock for CO2 geological storage purposes, Energy Procedia 4 (2011) 5422–5429.
[83] S.K. Haldar, Introduction to Mineralogy and Petrology, Elsevier, 2020.
[84] S. Iglauer, et al., CO2 wettability of caprocks: implications for structural storage capacity and containment security, Geophys. Res. Lett. 42 (21) (2015) 9279–9284.
[85] M. Arif, et al., Structural trapping capacity of oil-wet caprock as a function of pressure, temperature and salinity, Int. J. Greenh. Gas Contr. 50 (2016) 112–120.
[86] M. Arif, et al., Impact of pressure and temperature on CO2–brine–mica contact angles and CO2–brine interfacial tension: implications for carbon geo-sequestration, J. Colloid Interface Sci. 462 (2016) 208–215.
[87] V. Shah, et al., Water/acid gas interfacial tensions and their impact on acid gas geological storage, Int. J. Greenh. Gas Contr. 2 (4) (2008) 594–604.
[88] J. Wang, et al., Pore-scale modelling on hydrogen transport in porous media: implications for hydrogen storage in saline aquifers, Int. J. Hydrog. Energy 48 (37) (2023) 13922–13933.
[89] A. Al-Yaseri, et al., Snap-off effects and high hydrogen residual trapping: implications for underground hydrogen storage in sandstone aquifer, Energy Fuel 38 (4) (2024) 2983–2991.
[90] M. Bahrami, et al., Microfluidic investigation of pore-scale flow behavior and hysteresis in underground hydrogen storage in sandstones, J. Energy Storage 98 (2024) 112959.
[91] M.J. Shojaei, et al., Minimal surfaces in porous materials: X-ray image-based measurement of the contact angle and curvature in gas diffusion layers to design optimal performance of fuel cells, ACS Appl. Energ. Mater. 5 (4) (2022) 4613–4621.
[92] L. Hashemi, M. Blunt, H. Hajibeygi, Pore-scale modelling and sensitivity analyses of hydrogen-brine multiphase flow in geological porous media, Sci. Rep. 11 (1) (2021) 8348.